



HAL
open science

Structural health monitoring of civil engineering structures using GPR detection of patch antenna resonance frequency changes

Théo Richard, Amine Ihamouten, Mohamed Latrach, Xavier Dérobert, David Guilbert, Hartmut Gundel, Caroline Borderon

► To cite this version:

Théo Richard, Amine Ihamouten, Mohamed Latrach, Xavier Dérobert, David Guilbert, et al.. Structural health monitoring of civil engineering structures using GPR detection of patch antenna resonance frequency changes. IWAGPR 2019, Jun 2019, The Hague, Netherlands. hal-04296433

HAL Id: hal-04296433

<https://univ-eiffel.hal.science/hal-04296433>

Submitted on 20 Nov 2023

HAL is a multi-disciplinary open access archive for the deposit and dissemination of scientific research documents, whether they are published or not. The documents may come from teaching and research institutions in France or abroad, or from public or private research centers.

L'archive ouverte pluridisciplinaire **HAL**, est destinée au dépôt et à la diffusion de documents scientifiques de niveau recherche, publiés ou non, émanant des établissements d'enseignement et de recherche français ou étrangers, des laboratoires publics ou privés.

Structural health monitoring of civil engineering structures using GPR detection of patch antenna resonance frequency changes

Théo RICHARD
RF-EMC group
ESEO, IETR
Angers, FRANCE
theo.richard@eseo.fr

Amine IHAMOUTEN
ENDSUM / DTerO
Cerema
Angers, FRANCE
amine.ihamouten@cerema.fr

Mohamed LATRACH
RF-EMC group
ESEO, IETR
Angers, FRANCE
mohamed.latrach@eseo.fr

David GUILBERT
ENDSUM / DTerO
Cerema
Angers, FRANCE
david.guilbert@cerema.fr

Hartmut GUNDEL
IETR
Nantes University
Nantes, FRANCE
hartmut.gundel@univ-nantes.fr

Xavier DEROBERT
GeoEND/GERS
IFSTTAR
Nantes, FRANCE
xavier.derobert@ifsttar.fr

Caroline BORDERON
IETR
Nantes University
Nantes, FRANCE
caroline.borderon@univ-nantes.fr

Abstract—Wireless and inexpensive sensors present a great attractiveness and are of growing interest in such fields as civil engineering. In this study, the feasibility of a wireless sensing system, which consists of a patch antenna sensor and an external wireless interrogator, has been investigated. The patch antenna is designed to operate at two fundamental radiation modes (TM_{010} & TM_{001}) in the L Radar-frequency band according to the IEEE standard. The ground penetrating radar (GPR) interrogator consists of a printed Ultra-wide band Vivaldi antenna which is connected to a network analyzer. In order to evaluate its ability to monitor civil engineering structures, the performed patch antenna is placed behind various controlled slabs and its resonance frequency is varied artificially. The outside GPR interrogator permits to follow the frequency shift by measuring the reflected signal of the patch antenna. A series of preliminary experimental tests were carried out in order to demonstrate the principle.

Keywords—Monitoring, GPR, resonance frequency, concrete, patch antenna, wireless sensor, non-destructive testing.

I. INTRODUCTION

Civil engineering structures such as reinforced concrete in a maritime environment (either underwater or exposed to a tidal range), suffer from different environmental effects. Major damage may occur from water content with the ingress of chlorides while inducing rebar corrosion. Non-destructive testing (NDT) techniques have become a useful tool for engineers and structure owners in order to establish precisely monitoring [1-3]. Electromagnetic (EM) NDT techniques are sensitive to the presence of water and chlorides in concrete and also to porosity, mechanical NDT are sensitive to the mechanical properties of concrete structures [4-7]. Nevertheless, permanent monitoring is necessary, making wireless embedded sensors an extremely attractive means.

Therefore, the objective of the present study is to demonstrate that the frequency changes of an embedded sensor can be detected through the concrete structure by using an external interrogator. A patch antenna sensor has been chosen as a receiver/transmitter, in order to obtain a weak radiated electric field in the near-coupling area [8-9]. We are especially interested to minimize the concrete permittivity effect on the patch antenna characteristics. This will allow an efficient and unaltered signal transmission between the sensor and the external interrogator.

II. SETUP AND DEVICES

The wireless sensing system scenario, where the antenna sensor resonance frequency shift can be caused by various factors such as chloride ions ingress, as shown in Figure 1. For an unaltered transmission, the antenna sensor needs to be insensitive to the medium dielectric changes.

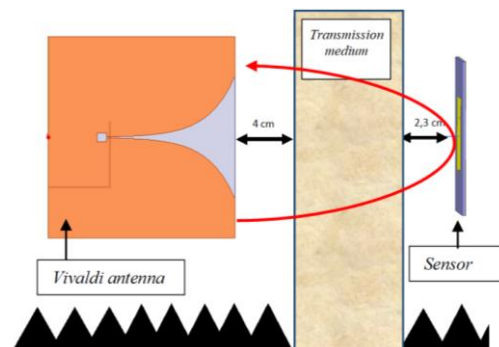


Fig. 1. Wireless sensing system scenario.

First of all, the signal level reflected by the antenna sensor needs to be sufficiently high, in order to allow proper identification of the antenna resonance frequency changes.

Secondly, the antenna sensor must be insensitive to the permittivity variations of the transmission medium. Actually, the properties of a material like concrete depend on the mixing characteristics, are influenced by the environment, and evolve during aging. Hence we discuss the aptitude to the sensor to be detected through any medium using an outside GPR interrogator. In order to imitate such varying properties, three different transition media (PVC, limestone, and concrete) with a relative permittivity ranging from 2.7 to 6.0 have been chosen.

Finally, three antenna sensors (same antenna with 3 different loads) were used in order to obtain three different resonance frequencies.

The detail of the antenna sensor's load design is not the scope of the present study. Instead, only the antenna sensor's state detection by an outside GPR interrogator must be studied.

A. Antenna sensor design and characterization

Depending on the dielectric properties of the surrounding medium, the reflection coefficient and radiation pattern of an antenna varies leading to a resonance frequency shift [9]. For this reason, a patch antenna has been chosen as it has a low electric near-field, which hence induces less coupling to a transition medium [8-10].

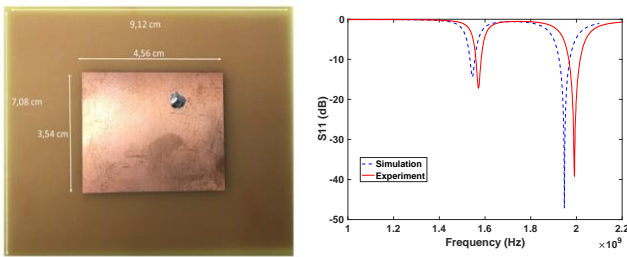


Fig. 2. Patch antenna (a) and HFSS simulation / experimental result of the input reflection coefficient (b).

The antenna geometry is shown in Figure 2a, designed to operate at two resonance frequencies of respectively 1.57 GHz and 1.99 GHz. Investigation of the transmission as a function of the concrete dielectric properties should allow revealing possible propagation differences between the two resonance frequencies. HFSS (High Frequency Structure Simulator) simulations and experimental measurements of the free space antenna input reflection coefficients are shown in Figure 2b. The difference between the simulation and measurement results is due to fabrication imperfections.

The antenna was separated from the transition medium by an air gap in order to prevent direct contact to the radiating element.

B. Optimization of the air layer thickness

The objective of this section is to define the optimal positioning of the antenna in front of the transmission medium in order to make it insensitive to the dielectric variations.

A simulation and experimental methodology was hence defined where the proposed patch antenna is placed in front of the transmission medium and progressively removed up to a distance of 5 cm. (distance d , see Figure 3). The dimensions of the coupling medium are $100 \times 100 \times 6 \text{ cm}^3$ and the analysis is done for the two adaptation frequencies of the antenna (Fig. 2b).

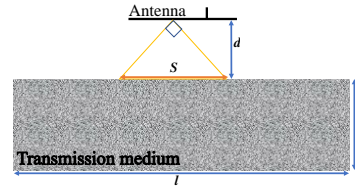


Fig. 3. Schema of the patch antenna in front of the dielectric transmission medium of different dielectric permittivities.

The results of the HFSS simulations are shown in Figure 4. Considering the frequency offset of the two resonance frequencies as a function of the air gap d (Figs. 4a and 4b), we observe a convergence of the two antenna resonance frequencies with the free space frequency (red curves) above 5 mm. At this distance, the resonance frequency variation is less than 1% in comparison to the red curves, for both frequencies and all studied media. An air gap of 5 mm thickness is hence necessary for minimizing the resonance frequencies offset.

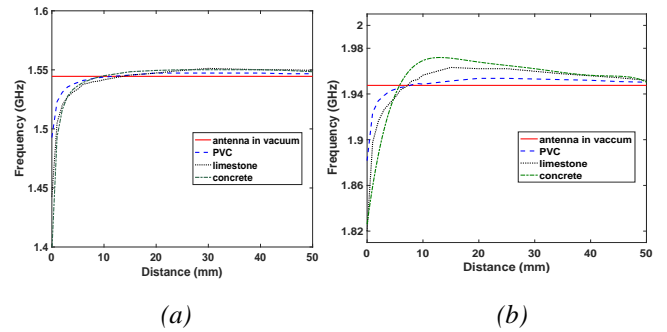


Fig. 4. Evolution of the simulated (HFSS) antenna resonance frequency vs. air gap thickness. First resonance frequency (a) and second resonance frequency (b) of the antenna for different dielectric media (ϵ_r PVC = 2.7, ϵ_r limestone = 4.5, ϵ_r concrete = 6.0).

The evolution of the measured antenna resonance frequency fluctuations according to the air gap thickness between the proposed antenna and the three controlled media is shown in Figure 5.

Both antenna resonance frequencies are compared respectively to the vacuum resonance frequency (indicated by the red horizontal curve). As for the simulation results (Fig. 4), the experimental curves show the same trends by crossing the vacuum resonance frequencies at a distance of approximately 5 mm. The frequency offset experimentally obtained is less than 1% with respect to the vacuum resonance frequency.

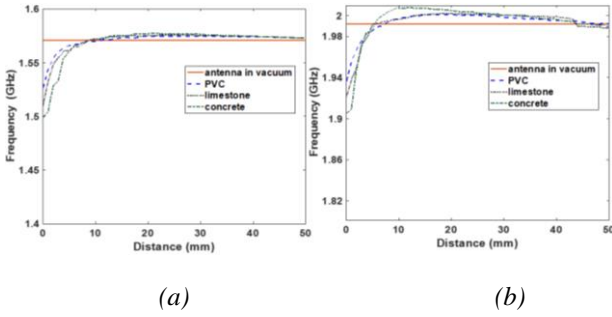


Fig. 5. Evolution of the experimentally obtained antenna resonance frequency as a function of the distance between the antenna and the transmission medium. First resonance frequency (a) and second resonance frequency (b) of the antenna for different relative permittivities ($\epsilon_r = 2.7, = 4.5, = 6.0$).

This study shows that the proposed configuration (patch antenna together with a 5 mm air gap) is robust against permittivity changes of the transmission medium. In the following, we propose to study the detection of the antenna resonant frequency through a limestone medium block.

III. USE OF AN OUTSIDE GPR FOR ANTENNA RESONANT FREQUENCY DETECTION

In this section, a load has been associated to the studied antenna in order to vary artificially its first resonance frequency. Objective is to follow the respective antenna frequency shift across a limestone medium block (Figure 6). For this, we use an outside GPR interrogator based on a stepped-frequency radar with an UWB Vivaldi antenna (effective frequency band: 0.8 GHz to 3 GHz with 1601 samples from a Vector Network Analyzer).

A. Experimental setup

Limestone is a very porous material (45-50 % porosity), with an important difference of the dielectric permittivity between its two hydric states (*i.e.* between $\epsilon_r = 4$ and $\epsilon_r = 18$ at 1.5 GHz).

Figure 6 shows the configuration which has been used for the experimental study. The dimensions of the tested limestone slabs are 100x100x6 cm³ (Figure 6).

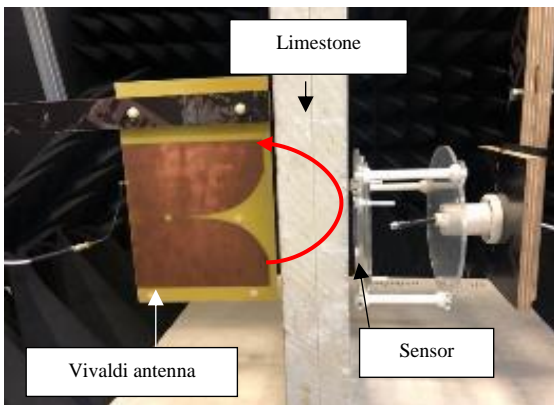


Fig. 6. Experimental measurement set-up.

The Vivaldi interrogator antenna is positioned at a distance of 4 cm from the front surface of the limestone block and the patch antenna is placed at 2.3 cm behind its back surface.

Antenna carriers have been used in order to accurately manipulate the positioning between the patch antenna, the Vivaldi antenna, and etalon slabs. The transmission medium chosen for this part of the study is dry/saturated limestone. The high difference in the respective complex permittivity and dispersion between the two hydric states in comparison with concrete allows imitating the extreme transmission conditions.

In order to allow analyzing of the resonance frequency of the patch antenna through the limestone medium, a calibration of the reflection interrogator GPR has to be done. The first antenna resonance frequency has been modified by varying the characteristics of the associated load.

B. Calibration procedure

The calibration was done by measurements using a metal plane instead of the patch antenna with their same dimensions and exact positioning. In the following, three different sensors of identical dimensions (same patch antenna but with 3 different loads) were used. The respective free space resonance frequencies are reported in Table 1.

TABLE I. SENSOR RESONANCE FREQUENCIES

	<i>Sensor 1</i>	<i>Sensor 2</i>	<i>Sensor 3</i>
Frequency	1.27 GHz	1.48 GHz	1.54 GHz

Signal processing is applied to the measured S_{11} coefficient of the Vivaldi antenna in order to extract the information on the sensor resonance frequency (Figure 7).

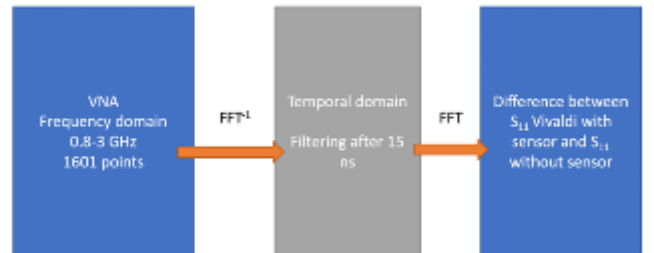


Fig. 7. Signal processing procedure

In the frequency domain, we apply the difference between the S_{11} parameters of the configuration Vivaldi / transmission medium / sensor or metal plane and Vivaldi / transmission medium / free space. In the rest of this article, this difference is noted as ΔS_{11} . This signal processing permits the extraction of the sensor signal absorption at the adaptation frequencies.

C. Results and discussion

In this section, we present and analyze the experimental results, allowing to follow the resonance frequency of the

patch antenna according to the three different loads (sensors 1, 2 and 3) and the two hydric states (dry and saturated) of the limestone media. These sensors act as a reflector of incident electromagnetic wave generated by the GPR interrogator. The signal analysis is hence done for the measured reflection coefficients at the input of the GPR Vivaldi Antenna.

Case 1: Dry limestone block

Figure 8 shows the ΔS_{11} signal measured by the outside GPR for the three sensors in the case of the Vivaldi antenna/sensor couple co-polarization operation and the first resonance frequency (Fig 8a) and the cross-polarization operation at the second resonance frequency (Fig 8b). The black arrows indicate the respective adaptation frequencies.

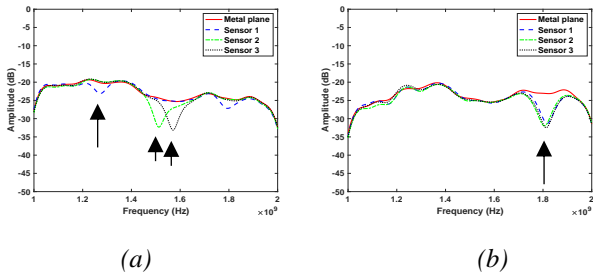


Fig. 8. Extracted GPR ΔS_{11} : (a) Co-polarization operation and (b) cross-polarization operation, in the presence of a dry limestone controlled block.

In Figure 8a a signal absorption loss at the respective resonance frequency of the three studied sensors can be seen. The observed attenuation of -3 dB to -6 dB (compared to the reference measurement with the metal plate) corresponds well to the sensor resonance frequency (see Table 1).

Figure 8b shows signal absorption at a frequency of 1.83 GHz. This corresponds to the second resonance frequency (TM₀₀₁ mode) identifiable only for perpendicular polarization (90 °) and which is constant whatever the sensor loads. This double sensor polarization is interesting for the calibration because it allows verifying the orientation and the exact positioning of the antenna in the structure.

In conclusion, we observe that it is possible to detect and to follow the working frequency (resonance frequency) of the sensors by an interrogator GPR in the case of a low permittivity transmission medium ($\epsilon_r = 4$).

Case 2: Wet limestone block

Figure 9 shows the ΔS_{11} signal measured by the outside GPR for the three sensor loads in the case of a saturated limestone block. The black arrows again indicate the corresponding resonance frequencies.

The results confirm those of the previous experimental study (Fig. 8) with a signal absorption loss at the resonance frequencies of the three studied sensors. The overall signal attenuation, however, is more important as the permittivity of the transmission medium is higher ($\epsilon_r = 18$). Nevertheless, it seems to be possible to detect and follow the resonance frequencies of the sensors with a GPR interrogator, too.

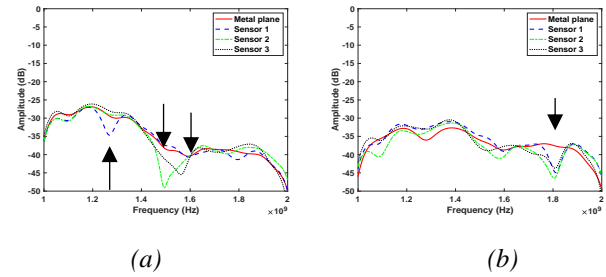


Fig. 9. Extracted GPR ΔS_{11} : (a) Co-polarization operation and (b) cross-polarization operation in the presence of a wet limestone controlled block.

IV. CONCLUSION

In this paper, we focused on the detection of different sensors by an outside GPR with an Ultra-Wide Band antenna. Two states of the transmission medium were represented by a limestone block either dry or wet. The tested sensor does not contain any electronics and has no alimentation. The outside GPR permits to follow the artificially induced frequency shift of the wireless sensor corresponding to a change in its adaptation characteristics, which could be provoked, for example, by the presence of chloride. Numerical and experimental parametric studies were done for the two controlled transmission medium states in order to validate the approach. It appears that detection and following of the adaptation characteristics of the sensor adaptation frequency by a GPR interrogator is possible whatever the dielectric and hence hydric state of the limestone medium block. The generalization approach to a concrete medium structure is in progress.

V. ACKNOWLEDGEMENTS

The present work has been performed in the frame of the research project *DADIM PdL* supported by the RFI WISE and the French region *Pays de la Loire*. The financial support is gratefully acknowledged.

VI. REFERENCES

- [1] J. H. Bungey and S. G. Millard, Testing of concrete structures, 3rd ed. Blackie academic & professional, Glasgow, 1996.
- [2] D. M. McCann and M. C. Forde, Review of NDT methods in the assessment of concrete and masonry structures, *NDT&E Int*, 2001, 71–84.
- [3] A. Ihamouten et al., Using machine learning algorithms to link volumetric water content to complex dielectric permittivity in a wide (33–2000 MHz) frequency band for hydraulic concretes, *Near Surf Geophys*, 2016, 527–36.
- [4] G. Villain et al., Determination of concrete water content by coupling electromagnetic methods: Coaxial/cylindrical transition line with capacitive probes, *NDT&E int*, 2017, 59–70.
- [5] J. Huginschmidt and R. Loser, Detection of chlorides and moisture in concrete structures with ground penetrating radar. *Mater Struct*, 2008, 785–92.
- [6] A. Kalogeropoulos, et al, Chlorides and moisture assessment in concrete by GPR full waveform inversion, *Near Surf Geophys*, 2011, 277–86.

[7]J. P. Balayssac et al., Description of the general outlines of SENSO project: Quality assessment and limits of different NDT methods, *Journ. Const. & Build. Mat.*, 2012, Vol. 35, pp. 131-138.

[8]C. A. Balanis, *Antenna theory: analysis and design*, John Wiley & Sons, 2016.